

## ASSESSMENT OF WAVE LOADS ON BRIDGE PIERS USING PHYSICAL AND NUMERICAL MODELLING

JULIEN SCHAGUENE<sup>1</sup>, THIBAUT OUDART<sup>2</sup>, BRUNO CHAFFRAIX<sup>3</sup>, OLIVIER BERTRAND<sup>4</sup>

*1 ARTELIA, France, julien.schaguene@arteliagroup.com*

*2 ARTELIA, France, thibault.oudart@arteliagroup.com*

*3 ARTELIA, France, bruno.chaffraix@arteliagroup.com*

*4 ARTELIA, France, olivier.bertrand@arteliagroup.com*

### ABSTRACT

The deep-water commercial port to be built, object of this paper, is an island port which will be served by a sea access bridge supported by piles. These piles are submitted to three types of forces: inertia forces, drag forces and wave breaking forces. As the first two type can be accurately approximated theoretically, the third one is highly dependent of the wave shape in the vicinity of the pile. As a consequence, in order to determine the hydrodynamic forces on the various piles of this bridge, a three-stages methodology was set up. An analysis of the loads was first carried out theoretically, the second stage consisted in carrying out physical model tests for a selected pile and in a third stage a numerical model was used. The paper will discuss the means and programme of the tests, and in particular the selection of characteristic waves and the results obtained.

**KEYWORDS:** wave load, numerical model, physical model, slamming load, vertical pile

## 1 INTRODUCTION

### 1.1 Generalities

The deep-water commercial port to be built, object of this paper, is an island port which will be served by a 1200 m long sea access bridge, supported by 300 piles, for land connection. The piles are arranged in 50 rows of 6 cylindrical piles of 1.5 m diameter and 4.5 m spaced. They are located on a seabed whose elevation varies between +2.0 m CD and -12.9 m CD.



Figure 1. Plan view of the bridge

In a previous mission, the sea states associated with return periods equal to 1 year and 200 years were propagated along the bridge assuming a unidirectional swell and without taking into account the masking effect of the port.

### 1.2 Methodology of the study

The piles are submitted to three types of forces: inertia forces, drag forces and wave breaking forces. As the first two type can be accurately approximated theoretically, the third one is highly dependent of the wave shape in the vicinity of the pile. Consequently, in order to determine the hydrodynamic forces on the various piles of this bridge, a three-stages methodology was set up:

- First, an evaluation of the loads was first carried out analytically,
- Then physical model tests for a selected pile were carried out, allowing to get a representative set of data, representative of different wave types;
- Finally, a numerical model was used, based on the data provided by physical model. This allows to calibrate numerical model parameters, and to apply them to other bottom level piles.

## 2 ANALYTICAL STUDY

An analysis of the loads was first carried out theoretically, based on a coastal wave propagation numerical model and literature formulae, like (1) and Figure 2. This stage led to an initial estimation of the loads, or at least a rough estimate, and contributed to the definition of the physical model to be set up (pile selection, scale choice, instrumentation requirements).

$$F = \frac{1}{2}\rho C_d D |U|U + C_m \rho A \dot{U} + \frac{1}{2}\rho D U^2 C_s \quad (1)$$

with  $U$  the velocity normal to the pile,  $\dot{U}$  the acceleration,  $C_d$  the drag coefficient,  $C_m$  the inertia coefficient and  $C_s$  the horizontal slamming coefficient. The two first terms are the non-breaking wave forces computed as the sum of the quasi static inertia and drag force whereas the last one is the impact force called slamming force.

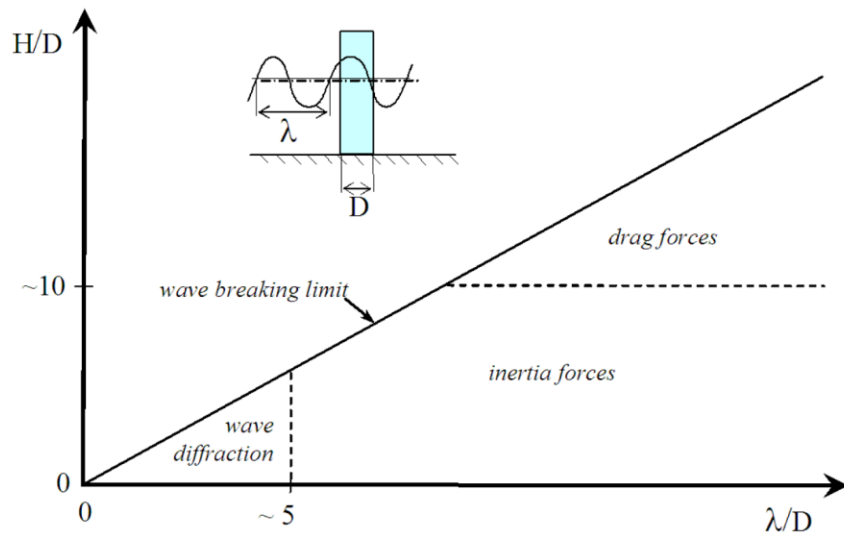


**Figure 2. Relative importance of inertia, drag and diffraction wave forces.**  
( $\lambda$  is the wave length,  $D$  is the diameter of the pile,  $H$  is the water depth) (DNV-OS-J101, 2010)

In our case of the maritime bridge piles ( $D = 1.5$  m), the wave height and wavelength vary between:  $H \approx 1$  m and  $\lambda \approx 50$  m, for the piles located at shallow depths to  $H \approx 10$  m and  $\lambda \approx 200$  m, for the piles furthest offshore. The study is therefore in a zone,  $H/D = [1 - 7]$  and  $\lambda/D = [30 - 130]$ , the inertial part of the forces is significant.

## 3 PHYSICAL MODELLING

### 3.1 Choice of the pile to be studied in wave flume

The piles are located in several bottom level, from -13mCD to +2mCD.

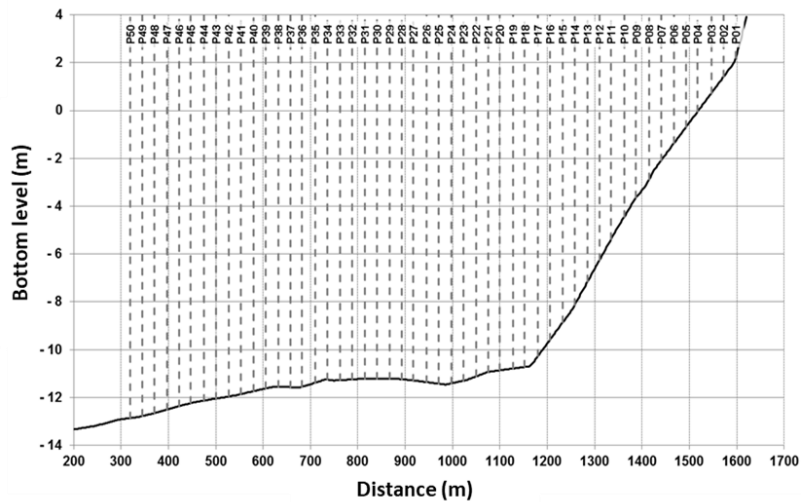


Figure 3. Bottom level of the piles

The final choice of pile and laboratory test conditions was made based on the simulation capabilities of the wave channel (scale) and the measurement equipment. For the study, it was decided to model pier #14 located at -8.1 m CD, which had been identified as being exposed to several types of wave impact. The wave conditions and levels established at this pile are as follows.

Table 1. Relevant conditions

N°	Return period	Still level [mCD]	Significant wave height $H_{1/3}$ (-8,5 mCD)[m]	Peak period $T_p$ [s]	$H_{max}$ [m]	Maximum level $N_{max}$ [mCD]	Minimum level $N_{min}$ [mCD]
1	1 year Low Water Level	-0,18	3.33	13.9	6.5	+4.02	-0.98
2	1 year High Water Level	+3,11	3.33	13.9	6.3	+7.64	1.84
3	200 years Low Water Level	-0,48	4.97	14.7	6.4	+3.3	-1.19
4	200 years High Water Level	+4,21	5.18	14.7	9.6	+9.8	+2.8

### 3.2 Wave flume

The tests were carried out at Artelia's hydraulic laboratory, in a wave flume measuring 41 m (22 m useful) x 1 m x 2 m. It is equipped with a wave generator with angular deflection. This wavemaker can generate regular or irregular waves, with a maximum significant wave height of 0.26 m and peak periods of between 0.7 and 3.5 s, for a maximum water height at the wavemaker of 1.4 m.

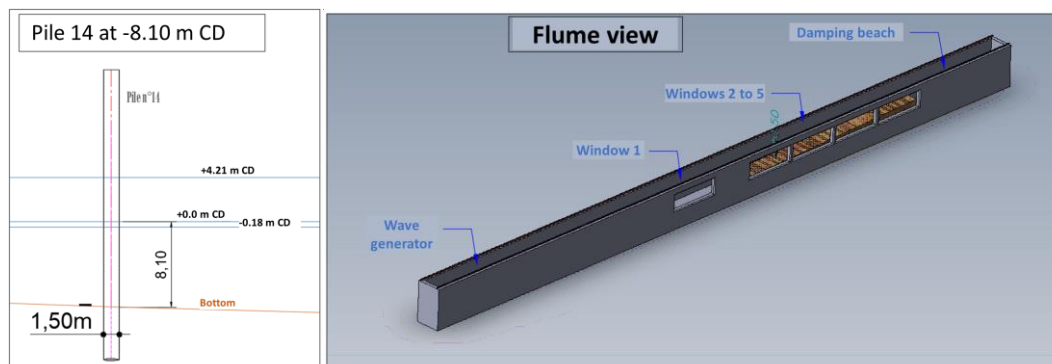


Figure 4. General view of the flume and pile being tested

### 3.3 The selected scale

The model is designed according to Froude's law of similarity as required by this type of structure which is subject to wave action. Froude's law consists of ensuring that the Froude number (ratio of inertial effects to gravity effects) on the model is equal to that in nature. The choice of model scale was guided by several constraints, and the  $E = 1/22$  scale was selected.

**Table 2. Table of conversion (for a seawater density of 1030 kg/m<sup>3</sup>)**

Physical quantity	Unity (SI)	Conversion ration (natural value / model value)
Length	m	S
Mass	kg	$1.03 * S^3$
Time	s	$\sqrt{S}$
Velocity	m / s	$S^{1/2}$
Acceleration	m / s <sup>2</sup>	1
Pressure	Pa	$1.03 * S * r$
Force	N	$1.03 * S^3$
Moment	N.m	$1.03 * S^4$

Note: \* r = 1 in the case of quasi-static pressures, and  $r = [0.1 - 1]$  according to the air entrapment mechanisms

### 3.4 The scale effects

The measured forces on the piles can be distinguish into 2 categories: impulsive forces and quasi static forces. It is necessary to be aware of the consequences of scale effects on each typology of forces.

#### 3.4.1 Impulsive forces

Since air cannot be scaled (identical compressibility in nature and in the model), it is generally recognised in the scientific community that impulsive forces are generally overestimated in a Froude model. This overestimation of forces depends on the air entrapment mechanisms observed on impact of the wave on the structure: the more complete the entrapment, the greater the overestimation of forces by Froude's law. A correction factor (r) can then be applied. For example, in the case of complete entrapment of the air, as it is sometimes observed when a wave plunges onto a vertical wall, the correction factor is  $r = 0.5$  for the scales considered, according to the law of compression (Cuomo et al., 2010). In the case of a cylindrical pile, we can expect the impulsive forces to be fairly representative (not overestimated). Observations of impacts in the laboratory confirm these results.

#### 3.4.2 Quasi-static forces

It is generally recognised by the scientific community that quasi-static forces are well represented in a Froude model. For the four sea states considered, the velocities of the water particles at the time of maximum stress exerted by the wave on the pile are estimated to be of the order of 2 m/s (bottom) to 7 m/s (top), according to Fenton's theory. The associated Reynolds numbers are of the order of 20,000 to around 120,000 at 1/22, which makes it possible to maintain a turbulent medium at the scale of the pile and to limit viscous scale effects. On the other hand, the dimensionless numbers KC and  $\beta = Re / KC$  respectively vary between:  $KC = [1 - 2]$  and  $\beta = [20,000 - 70,000]$  at the model scale, against  $KC = [20 - 35]$  and  $\beta = [90,000 - 320,000]$  at the natural scale. By extrapolation of the Sarpkaya (1976) charts, there will be a slight overestimation of the drag forces in the Froude model. Inertial forces, on the other hand, will be faithfully represented.

### 3.5 Measurement equipment

The pile was equipped with 13 pressure sensors and a force balance. A focus was made over the risk of specific frequency excitation, regarding the measurement equipment. Quasi-static wave excitation frequencies are around 0.5 Hz and 5 Hz, i.e. outside the resonance zone of all the sensors. Impulsive wave excitation frequencies ranged from  $f = 50$  to 500 Hz, which is below the natural frequency of the sensors ( $F = 90,000$  Hz) located on the front of the pile, where slapping could occur. Pressures were measured at an acquisition frequency of between 1000 and 5000 Hz (model) in order to record impulsive and quasi-static stimulation.

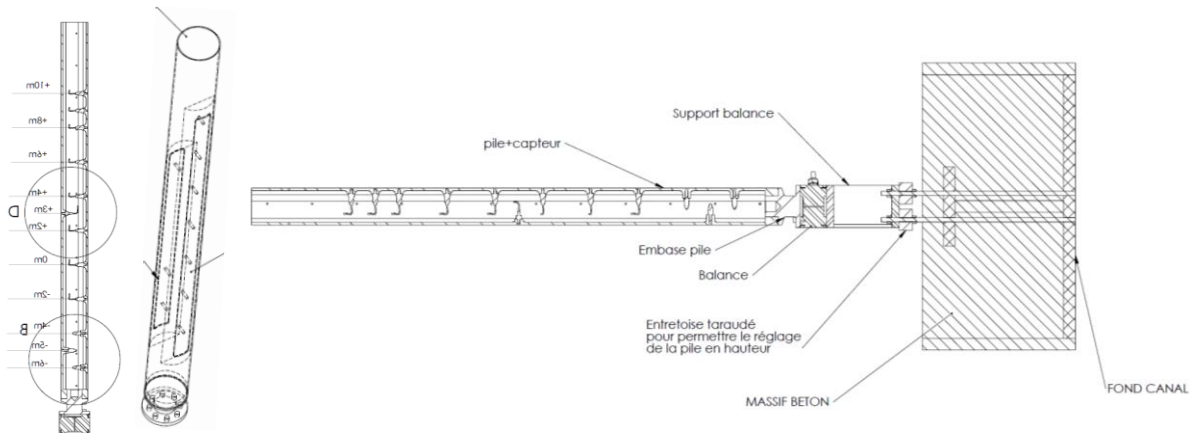


**Figure 5. Plan of the pile and its position in the wave flume**

### 3.6 Spectral wave generation

The test programme begins with spectral wave tests. The programme described in Table 1 is first used to calibrate the wave conditions without the pile. Then, the pile is added to the wave flume and the wave time series are played again to measure the forces on the pile. In this stage, wave loads were measured on the pile for different types of waves (unbroken, broken and breaking) corresponding to annual and two-hundred-year storms, low and high water level. The modelled pile, was exposed to maximum loads that could reach between 500 kN and 1,500 kN, including 300 to 1,000 kN of impulsive type; the maximum pressure estimated at the level of the impact zone being approximately 500 kN/m<sup>2</sup>. Impulsive and non-impulsive forces are simulated for each sea state and considering a non-breaking wave, a breaking wave and a broken wave (if observed in the laboratory). A total of 9 waves were studied.



**Figure 6. Non breaking wave, breaking wave, and broken wave examples**

These different type of waves shows different pressure measurement patterns. It can be majorly quasi static forces for a non-breaking wave (Figure 7 – Highest wave recorded) or majorly impulsive forces for a breaking one (Figure 8 – Highest load recorded).

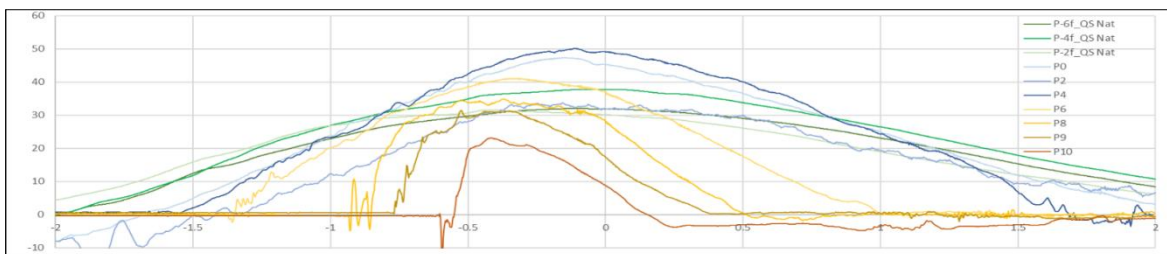


**Figure 7. Pressure time series for the highest wave selected  $H = 9.7\text{m}$   $T=10.4\text{s}$**

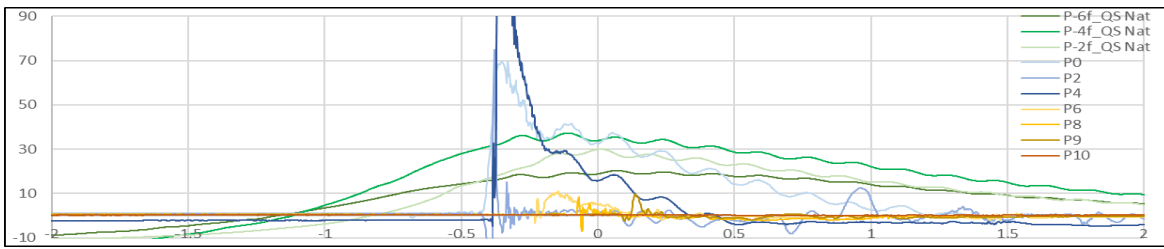


Figure 8. Pressure time series for highest load measured & highest impulsive pressure (H = 6.8m T=15.9s)

### 3.7 Bi chromatic wave generation

As the numerical simulation of spectral generated waves was not possible at the time of the study (simulation times would have been too long), the objective of this phase is to reproduce specific waves identified previously with only a bi chromatic wave generation. These specific waves can next be simulated with numerical model. An iterative process is followed to reproduce the special features of each of the selected waves. A focus is made on wave height, period, overall load, maximum pressure location and intensity. The forces and pressures are generally well reproduced in bichromatic mode, with a slight tendency to underestimate them (Figure 9).

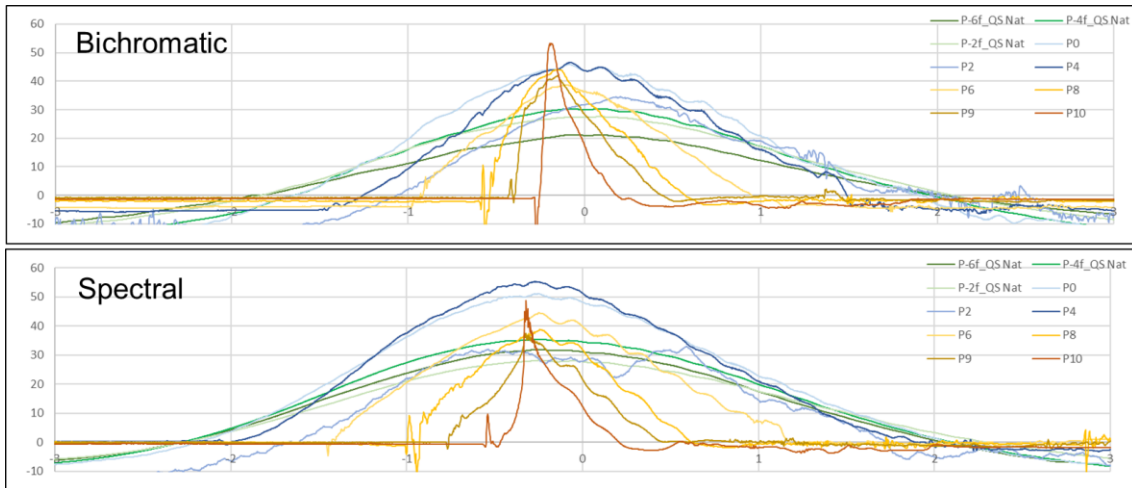


Figure 9. Comparison between pressure time series for bichromatic and spectral mode for non impulsive wave

Generally, this reproduction is quite accurate for non-impulsive waves (Figure 10).

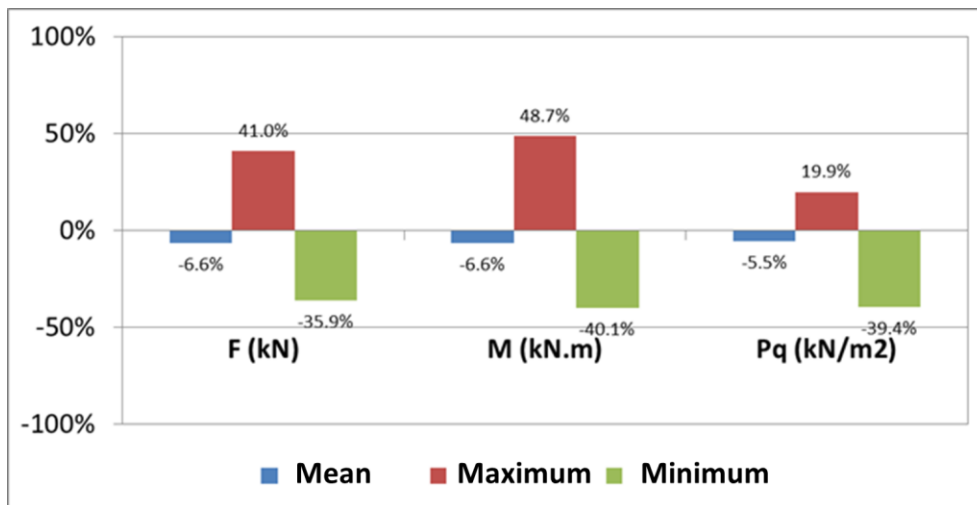


Figure 10. Difference for notable values between bichromatic mode and spectral mode for non impulsive waves

However, for some of the identified waves, notable differences are measured in the impulsive component of the force

(Figure 11, Figure 12), despite a good correspondence of heights and periods between the bi-chromatic mode and the spectral mode; which is probably attributable to the detail of the shape of the wave at the time of impact on the pile (detail not characterizable in the tabulated parameters H, T, breaking mode). For certain waves, it was not possible to reproduce the impulsive feature of some of the waves in simple bi-chromatic mode. Without doubt, this is one of the limitations of wave flume tests.

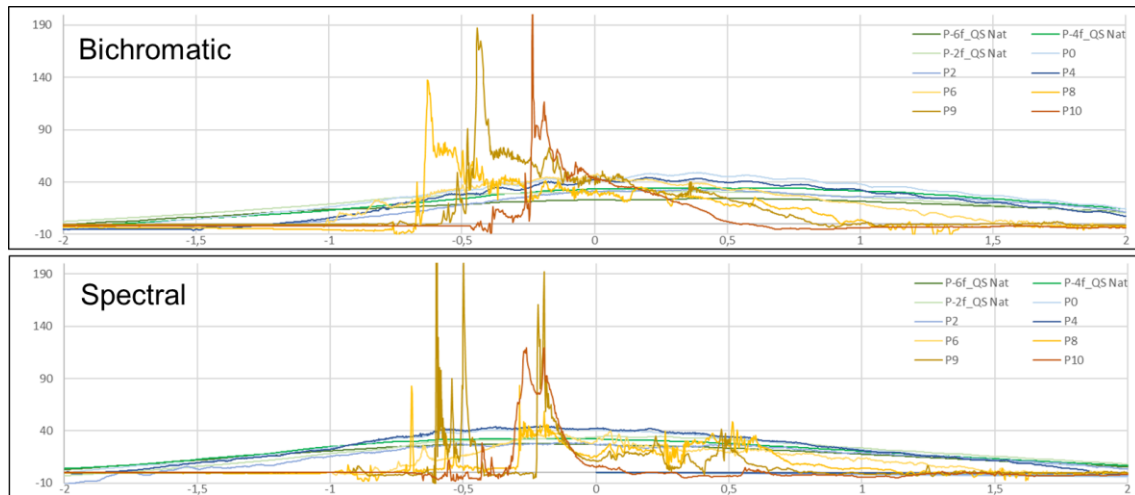


Figure 11. Comparison between pressure time series for bichromatic and spectral mode for impulsive wave

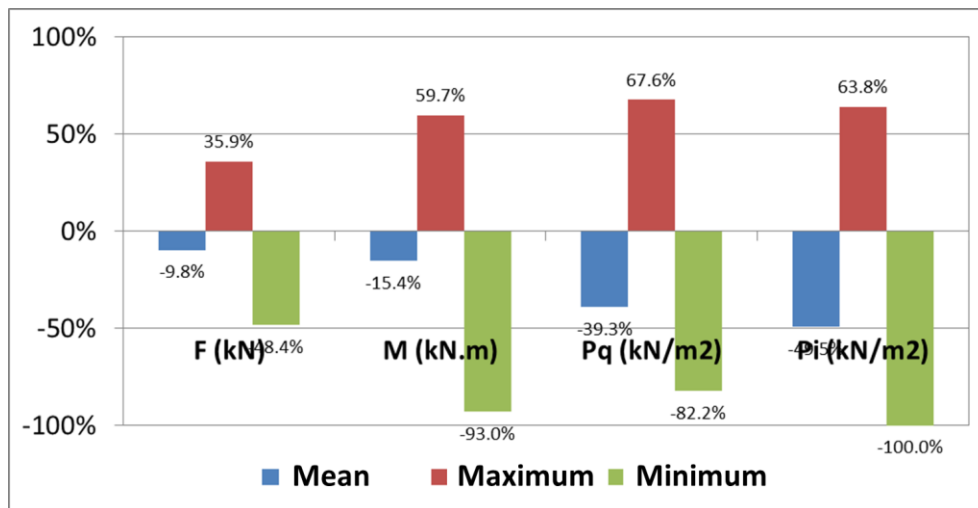


Figure 12. Difference for notable values between bichromatic mode and the spectral mode for impulsive waves

#### 4 NUMERICAL MODELLING

During this third stage, a numerical model of the same pile studied on the physical model was set up, calibrated with the results of the physical model. The calibrated numerical model was then used on a pile located in a deeper zone where wave breaking is infrequent and on a pile located in a shallower zone where wave breaking is predominant.

##### 4.1 Numerical model description

The numerical study is based on a numerical modelling developed using OpenFOAM software. The OpenFOAM three-dimensional computational code solves the Reynolds equations, which correspond to the Navier-Stokes equations in the turbulent regime. These RANS (Reynolds Average Navier-Stokes) equations govern the transport of mean flow quantities and model all scales of turbulence. There is no universality in terms of turbulence modelling. For this study, a standard model is used, with the 2 equations k- $\omega$  model (k: turbulent kinetic energy and  $\omega$ : specific dissipation). These are certainly the most widely used models today. The dimensions of the model are similar to those of the physical wave flume. It is meshed with around 800'000 cells, in particular in the vicinity of the pile.

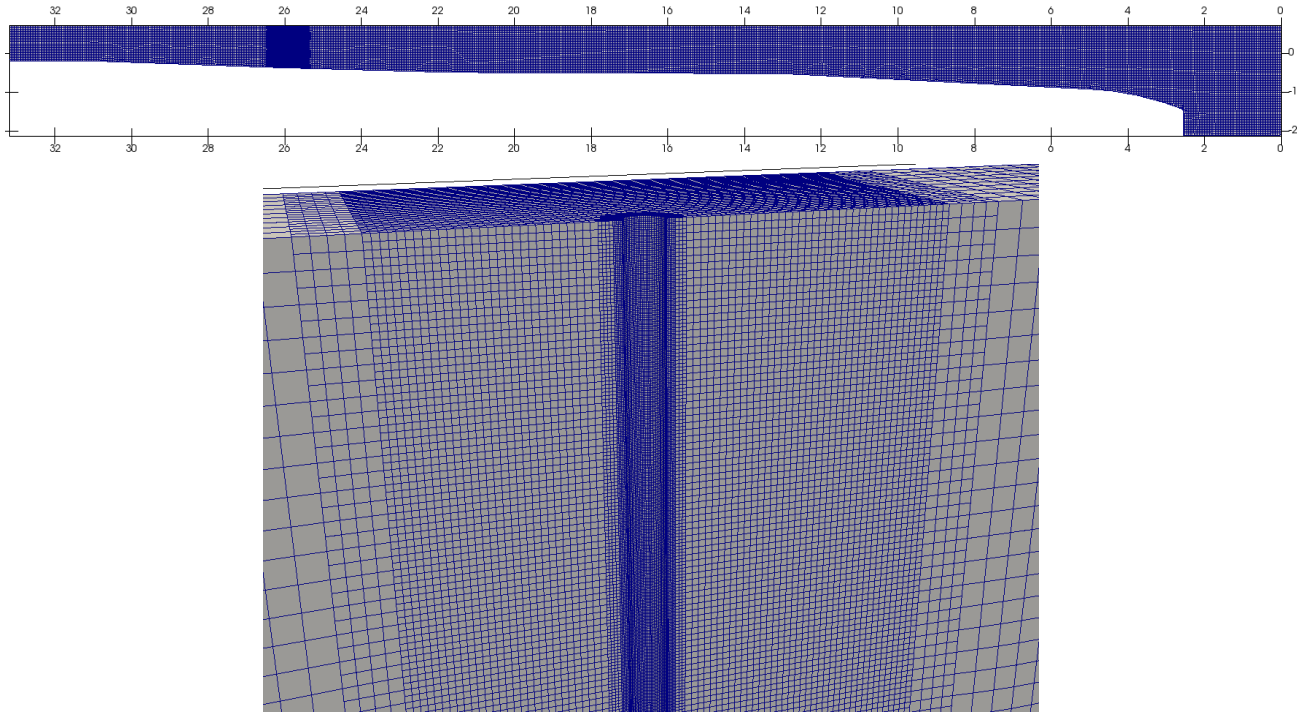


**Figure 13. Vertical cut of the mesh in the overall flume (up) and in the vicinity of the pile (bottom)**

#### **4.2 Reproduction of waves identified in the physical wave flume**

The waves are reproduced in simple mode (monochromatic or bi-chromatic) and their calibration is carried out by modifying the wave generation parameters, the turbulence level and the courant number, also known as the CFL condition in order to obtain the range of forces measured in the wave channel. Impulsive and non-impulsive modes are simulated for each sea state, taking into account a non-breaking wave, a breaking wave and an already broken wave (if observed in the laboratory). The following table shows the range of forces and pressures obtained in the numerical flume. The accuracy of the numerical model is generally around +/-20% for the peak force measurements and +/- 5% for the wave height measurements.

**Table 3. Range of forces and pressures obtained in both models**

<b>Model</b>	<b>Effort</b>	<b>Moment</b>	<b>Impacting pressure</b>	<b>Quasi-static pressure</b>
	<b>Kn</b>	<b>Kn.m</b>	<b>kPa</b>	<b>kPa</b>
Numerical model	112 - 776	2 100 - 11 780	122 - 875	7 - 200
Physical model	122 - 781	1 172 - 11 141	143 - 852	32 - 162

The following figures show some details of the pressures exerted by the waves on the sensors located on the front of the pile.



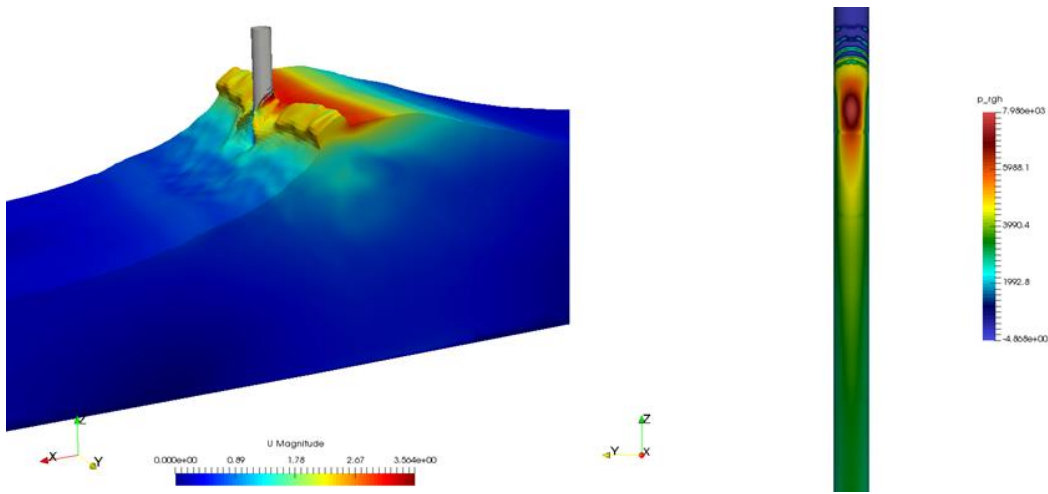


Figure 14. Pressure distribution for the highest wave (H = 9.6 m, Tz = 10.5 s, F = 356 Kn)

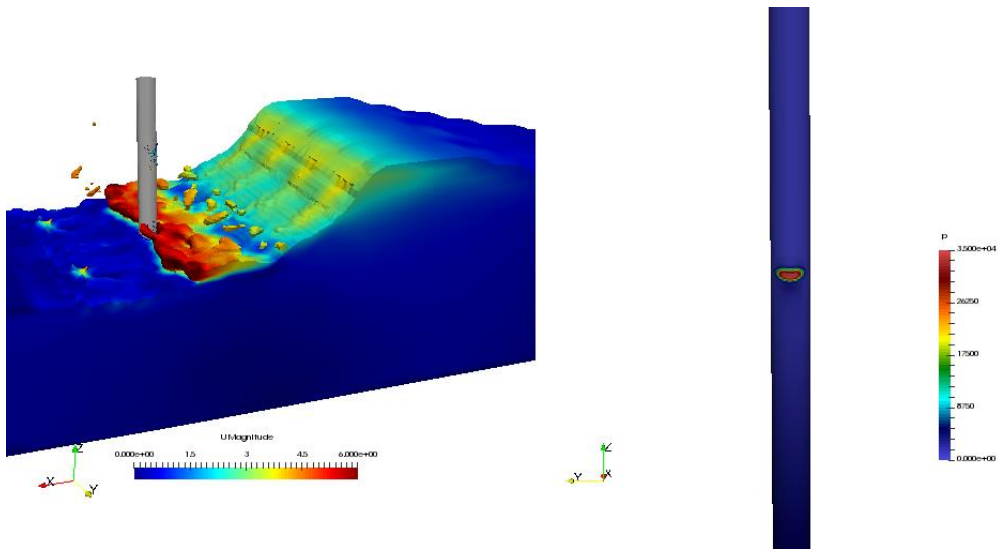


Figure 15. Pressure distribution for the lowest wave (H = 7.4 m, Tz = 12 s, F= 560 Kn)

### 4.3 Simplified methodology for forces estimation

Following the reproduction in numerical model of specific waves, the initial formula (1) is modified to:

$$F = \int \frac{1}{2} \rho C_d D |U| U dz + C_m \rho A U \dot{z} + \frac{1}{2} \rho D U^2 C_s dz \quad (2)$$

with  $U$  the velocity calculated by CFD model,  $D$  the pile diameter,  $Dz$  the vertical discretisation of the pile.

The  $C_d$  drag coefficient,  $C_m$  inertia coefficient and  $C_s$  horizontal slamming coefficient are estimated thanks to the results of physical model.

### 4.4 Estimation of the forces on other piles using numerical model

The numerical model is then used to estimate the forces in two other characteristic zones of the bridge. The forces are then compared to those calculated by the formula (2)

#### 4.4.1 High depth pile

On a pile located at a high depth, waves break rarely due to the effect of depth (breaking rate less than approximately 1%)

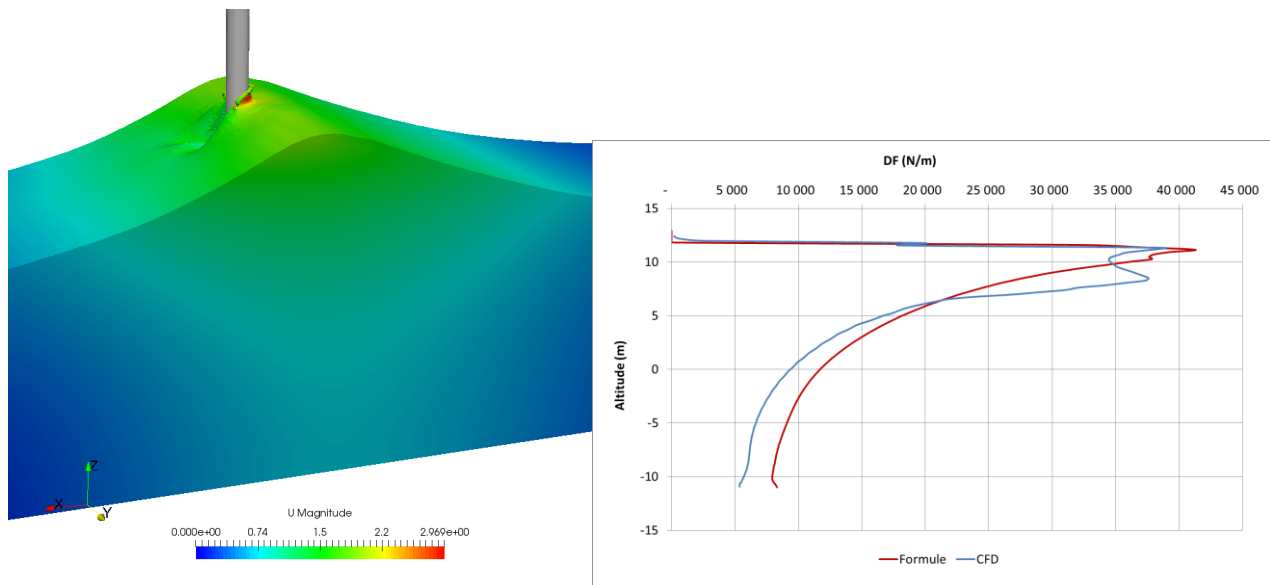


**Figure 16. Pressure distribution for a non-breaking wave ( $H = 9.5$  m,  $T_z = 14.7$  s,  $F = 342$  Kn)**

In the graph on the left, the coefficients are adjusted so that the empirically calculated vertical distribution of force conforms to the vertical distribution estimated from the numerical model.

#### 4.4.2 Shallow depth pile

On a pile located at a very shallow depth, most of the waves break and the turbulence rate is very high (breaking rate greater than around 95%).

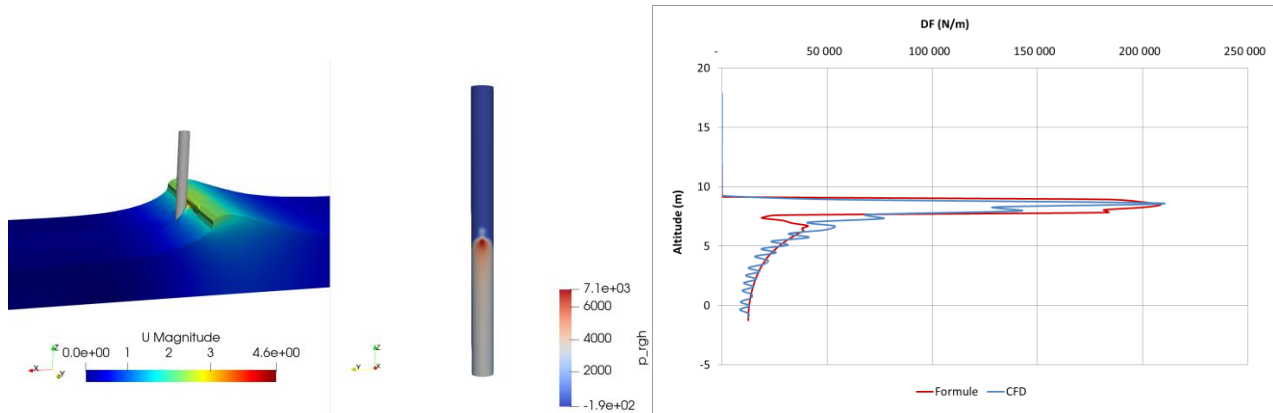


**Figure 17. Pressure distribution for the highest wave ( $H = 5.4$  m,  $T_z = 11.0$  s,  $F = 396$  Kn)**

This approach shows the relevance of using the two modelling tools, which can complement each other on a number of issues.

## 5 CONCLUSIONS AND FURTHER RESEARCH

The study presents the development of an innovative methodology for calibrating the parameters of a numerical model of bridge piles subjected to waves. This is based on simulation realized over a physical model, allowing the acquisition of an accurate and complete data set to cover a large number of hydraulic situations. This data set makes it possible to reliably calibrate the numerical model, which can then be applied to pile located at any water depth. This approach has the advantage of allowing the reproduction of wave forces on piles of great depth or very shallow depth, for which a physical model would remain very complicated to realize due to the size of the infrastructures and the scale effects.

One of the most tedious stages of the process was the reproduction of spectral phenomena in bi-chromatic generation, on the scale model, in order to simplify the generation in numerical modeling subsequently. As spectral phenomena are composed of multiple characteristics, it was complicated to repeat these phenomena with only two components, and differences appeared at this stage. In the future, we plan to develop a new methodology, similar to that presented here, but without the stage of simplifying the generation signal. The waves identified during the spectral generation will be replayed directly in the numerical model with the characteristics of all their components, taking into account around ten previous waves

so that the sea state of the numerical wave flume is similar to that of the physical wave flume. This will make it possible to overcome the approximation induced by the bichromatic approach.

Also, this study does not make it possible to evaluate group effects and interactions between piles. To do this, it would be necessary to model a set of instrumented piles in the laboratory, but this can only be done with infrastructure larger than a wave flume, also making it possible to evaluate the impact of the wave incidence on sets.

## REFERENCES

DNV-OS-J101, 2010

Giovanni Cuomo, William Allsop, Shigeo Takahashi, 2010, Scaling wave impact pressures on vertical walls, *Coastal Engineering*, volume 57, pages 604–609.

Fenton, J.D. 1990, Nonlinear Wave Theories, *The Sea, Vol 9: Ocean Engineering Science*

Sarpkaya, T. (1976). Forces on rough-walled circular cylinders. *Coastal Engineering Proceedings*, 1(15), 134.